

# Petrology of a dolerite in Netherlands offshore well G/17-2

R.P. Kuijper

Kuijper, R.P. Petrology of a dolerite in Netherlands offshore well G/17-2. – Scripta Geol., 96: 33-46, 2 figs., 1 pl., December 1991.

A dolerite intrusion in Upper Carboniferous sediments in Netherlands offshore block G/17 is described. Based on electron microprobe analyses of clinopyroxene and olivine, a minimum temperature of emplacement of some 1000°C is calculated. As a result of the intrusion, the maturation profile of the surrounding sediments may show a departure from linear behaviour.

R.P. Kuijper, Satijnvlinder 20, 2317 KJ Leiden, The Netherlands, and National Museum of Natural History, Postbus 9517, 2300 RA Leiden, The Netherlands.

---

Introduction	33
Geological setting	35
Acknowledgements	35
Petrography	35
Description of constituent minerals	37
Mineral composition	38
Mineral composition and emplacement of the dolerite	41
Thermal disturbance of the surrounding sediments	43
Discussion	44
References	45

---

## Introduction

The exploration well G/17-2 was drilled in 1984-1985 in Netherlands offshore block G/17, some 70 km north of the isle of Terschelling. Circa 300 m below the top of the Upper Carboniferous, a 14 m thick section of dolerite was encountered. A limited petrographical and petrological study was performed on the well-cuttings, no cores or side-wall samples having been taken over the interval.

Igneous rocks have received only limited attention in the petroleum industry, in Western Europe in particular. Widespread volcanics are being used as stratigraphic marker-horizons, and in some instances fractured igneous rocks have been recognized as possible reservoirs, but a full use of petrological and geochemical

data on igneous rocks has hardly been attempted. This is due partly to sampling methods and sample size, which normally preclude meaningful geochemical and isotope analysis. Especially in a complex evolution, like the one pertaining to the sedimentary basins of Western Europe, igneous rocks can provide valuable insights and constraints.

Apart from the widespread Dongen Tuffite of Eocene age, only a limited number of occurrences of igneous rocks have been described from the Dutch subsurface (Table 1). Phonolites, trachytes, leucite-phonolites, and phonolitic basanites have been encountered in the onshore well Zuidwal #1; these rocks have revealed a  $^{40}\text{Ar}/^{39}\text{Ar}$  age of  $144 \pm 1$  Ma (Dixon et al., 1981) and a  $^{40}\text{Ar}/^{36}\text{Ar} - ^{40}\text{K}/^{36}\text{Ar}$  age of  $152 \pm 3$  Ma (Perrot & van der Poel, 1987). Other undersaturated alkaline rocks include the nephelinites and basanites of onshore wells Andel #2, Andel #4 and Loon op Zand #1, the basaltic rocks of offshore wells K/14-FA103, L/13-3 and Q/7-2, and the lamprophyres of wells F/10-1, K/12-5 and P/6-B1. Felsic (sub)volcanic rocks (rhyolites and micro-granodiorites) occur in the northern part of the Dutch offshore (wells A/15-1, A/17-1, F/4-2). Highly altered mafic rocks have been described from onshore wells Wanneperveen #1 (dolerites and olivine-gabbros),

Table 1. Igneous rocks in The Netherlands.

Well	Stratigraphic interval	Rock type	Isotopic age (Ma)
Andel #2, #4	Middle Jurassic	nephelinites, basanites <sup>1</sup>	$133 \pm 2$
Berkel #1	Jurassic (?)	Hbl-basalt <sup>4</sup>	
Loon op Zand #1	Middle Jurassic	nephelinites, basanites <sup>1</sup>	$132 \pm 3$
Oldenzaal #2	Upper Jurassic (Wealden)	Hbl-dolerite <sup>5</sup>	
Wanneperveen #1	Lower Permian	dolerites, (Ol-)gabbros <sup>2</sup>	
Zuidwal #1	(pre-)Valanginian	phonolites, trachytes, leucite-phonolites, phonolitic basanites <sup>1</sup>	$144 \pm 1$ $152 \pm 3$
A/15-1	Rotliegend	gabbro, micro-granodiorite <sup>3</sup>	
A/17-1	Palaeozoic	rhyolite <sup>3</sup>	
F/4-2a	Rotliegend	micro-granodiorite <sup>3</sup>	
F/10-1	Zechstein	lamprophyre <sup>3</sup>	
K/12-5	Zechstein	lamprophyre <sup>3</sup>	
K/14-FA103	Lower Permian	trachybasalt <sup>1</sup>	
L/13-3	Zechstein	Ol-nephelinite <sup>1</sup>	100 - 110
P/6-B1	Triassic	lamprophyre <sup>3</sup>	
Q/7-2	Triassic	undersaturated basalt <sup>1</sup>	92 - 107

<sup>1</sup> Dixon et al., 1981; <sup>2</sup> Kimpe, 1953; <sup>3</sup> Kuijper, unpublished data; <sup>4</sup> van der Sijp, 1953; <sup>5</sup> Voort-huysen, 1944.

Oldenzaal #2 (hornblende-dolerite) and Berkel #1 (hornblende-basalt). Dixon et al. (1981) interpret part of these as undersaturated basaltic rocks (essexites, theralites). A much less altered gabbro occurs in well A/15-1, together with the micro-granodiorite forming a bimodal suite. A basement granite with a biotite  $^{40}\text{Ar}/^{39}\text{Ar}$  age of 346 Ma was encountered at total depth in well A/17-1.

#### GEOLOGICAL SETTING

Block G/17 is situated on the platform area east of the Dutch Central Graben. In this area sediments of the Limburg Group of mainly Westphalian age are overlain by a thick section of Permian Rotliegendes and Zechstein claystones and evaporites, deposited in the central parts of the Southern Permian Basin.

Triassic and Jurassic sediments are thinly developed or absent due to erosion and/or non-deposition. Sedimentation resumed in the Cretaceous and thick sections of Upper Cretaceous chalk and Tertiary through Quaternary clays and sands are present all over of the area (NAM & RGD, 1980).

#### ACKNOWLEDGEMENTS

The author is indebted to Mobil Producing Netherlands Inc. and to Holland Sea Search Holding N.V. for permission to publish this report. Electron microprobe analyses were performed by Dr P. Maaskant at the electron microprobe laboratory of the Instituut voor Aardwetenschappen, Vrije Universiteit, Amsterdam, with financial and personnel support by N.W.O.-W.A.C.O.M. (research group for analytical chemistry of minerals and rocks subsidized by the Netherlands Organization for the Advancement of Pure Research). The comments and criticism of Dr C.E.S. Arps, which greatly improved the manuscript, are gratefully acknowledged.

### Petrography

Macroscopically, the G/17-2 dolerite is green to grey coloured and fine to very fine grained. Feldspar can be identified, but the mafic minerals cannot be distinguished separately.

Microscopically, the dolerite shows a typical (sub)ophitic texture, made up of elongated feldspar laths and anhedral pyroxene and olivine (Pl. 1, fig. 1). No preferred mineral orientation can be discerned on the scale of the samples, all crystals being randomly oriented.

In view of the generally undeformed aspect of the rock and the absence of deformation textures, local undulatory extinction of plagioclase and pyroxene is probably due to bit-metamorphism, an artefact of the drilling process (Taylor, 1983). Main constituents are plagioclase (50%), clinopyroxene (40%) and olivine (10%). Minor and accessory minerals are sphene, opaque minerals and zircon. Reaction products are biotite, sericite, chlorite, and serpentine.

In view of the presence of olivine in all of the samples, the accessory quartz is probably related to assimilated wall-rock.



## Plate 1

Fig. 1. G/17-2 dolerite, overview,  $\times 63$ , PPL.

Fig. 2. G/17-2 dolerite, vein filled with microcrystalline biotite crosscutting dolerite,  $\times 63$ , PPL.

## DESCRIPTION OF CONSTITUENT MINERALS

*Main constituents*

*Plagioclase* has an An-content of 40-50%, based on optical properties, and occurs as anhedral-subhedral, elongated to stubby grains. Twinning is mainly according to the Albite and Pericline laws. Especially the larger grains show a strong optical zonation, reflecting changes from an An-rich core to an Ab-rich rim. Alteration is absent in most samples, but locally sericite-aggregates partially replace plagioclase.

Based on its optical properties, the *clinopyroxene* is rich in diopside – aegirine-augite (greenish with only weak to very weak pleochroism from colourless to very light green ( $\alpha$ ) to pale green ( $\gamma$ );  $2V_{\gamma} = 60-80^{\circ}$ ,  $r > v$  weak to moderate,  $V_{\gamma} \wedge C 30-40^{\circ}$ ). Clinopyroxene occurs as anhedral grains between plagioclase laths, often in optical continuity, and locally poikilitic with plagioclase-inclusions. Alteration is strongly variable, in extent as well as in products. In all samples, local development of biotite after clinopyroxene is apparent. Other alteration products are micro- to cryptocrystalline sericite/chlorite aggregates.

The *olivine* has a Fo-content of 60-80%, based on its optical properties (colourless,  $2V_{\alpha} = 80-90^{\circ}$ ) and occurs as anhedral to subhedral grains, locally somewhat corroded. Olivine is mostly mantled by a rim of micro- to cryptocrystalline alteration products (serpentine and/or chlorite).

*Minor and accessory minerals*

*Sphene* occurs as tiny, anhedral grains in more or less elongated aggregates. *Opaque minerals* occur as tiny inclusions along cleavage-planes in clinopyroxene, as tiny grains within sericite/chlorite/serpentine aggregates, and as larger anhedral grains, interstitial in the plagioclase-clinopyroxene matrix. One single grain of *zircon* was encountered in only one sample.

*Alteration products and post-emplacement mineralizations*

*Biotite* is strongly pleochroic, light brown to brown, and is mostly not well crystallized. It occurs as very fine grained polycrystalline to microcrystalline aggregates as rims along, and overgrowths on, clinopyroxene, partially to completely replacing it, locally together with chlorite. Microcrystalline biotite in combtexture occurs as vein-filling material (Pl. 1, fig. 2) in one sample, together with possible *prehnite*. *Sericite* occurs as micro- to cryptocrystalline aggregates at the expense of plagioclase, and together with chlorite at the expense of clinopyroxene. The *chlorite* is pleochroic green and occurs within micro- to cryptocrystalline biotite-chlorite aggregates after clinopyroxene and together with colourless *serpentine* in micro- to cryptocrystalline aggregates after olivine. Locally *calcite* forms overgrowths on plagioclase.

From textural observations it is clear that the dolerite intruded as a dyke or sheet, some time after the deposition of the Upper Carboniferous sediments. The limited amount of samples available and the sampling method preclude the assess-

ment of presence or absence of chilled rim zones. As most of the dolerite is essentially unaltered, even along local biotite (hence fluid-rich) veins, the limited replacement of the original igneous paragenesis probably relates to low-T alteration effects upon the introduction of fluids along cracks (veining) or along crystal-boundaries.

#### MINERAL COMPOSITION

##### *Pyroxenes*

Table 2. Clinopyroxene composition and end-member ratios.

	CPX-A	CPX-B	CPX-C	CPX-D	CPX-E
Wt.% oxide					
SiO <sub>2</sub>	50.00	50.50	50.70	51.30	50.90
Al <sub>2</sub> O <sub>3</sub>	3.18	2.83	2.65	2.91	2.79
TiO <sub>2</sub>	1.04	1.18	1.12	0.92	1.11
Cr <sub>2</sub> O <sub>3</sub>	0.15	0.00	0.00	0.11	0.06
FeO	8.48	11.70	12.00	9.14	10.10
MnO	0.20	0.27	0.34	0.23	0.26
MgO	14.50	15.30	15.80	15.30	15.30
CaO	20.30	17.30	16.60	19.80	18.90
Na <sub>2</sub> O	0.28	0.32	0.29	0.32	0.33
Total	98.13	99.40	99.50	100.03	99.75
Atomic ratios					
Si	1.890	1.893	1.897	1.900	1.895
Al <sup>IV</sup>	0.110	0.107	0.103	0.100	0.105
Al <sup>VI</sup>	0.032	0.018	0.014	0.027	0.018
Ti	0.030	0.033	0.032	0.026	0.031
Cr	0.005	0.000	0.000	0.003	0.002
Fe <sup>3+</sup>	0.035	0.045	0.047	0.041	0.047
Fe <sup>2+</sup>	0.233	0.322	0.329	0.242	0.267
Mg	0.817	0.855	0.881	0.845	0.849
Mn	0.006	0.009	0.011	0.007	0.008
Ca	0.822	0.695	0.666	0.786	0.754
Na	0.021	0.023	0.021	0.023	0.024
End-member %					
Ti-Diopside	2.95	3.33	3.15	2.56	3.11
Aegirine	2.05	2.33	2.11	2.30	2.39
Tschermakite	5.08	4.03	3.96	4.85	4.27
Hedenbergite	23.30	32.15	32.90	24.21	26.73
Diopside	50.89	29.99	26.54	46.96	41.29
Kanoite	0.64	0.86	1.08	0.72	0.82
Clinoenstatite	15.09	27.32	30.26	18.40	21.40

End-member compositions used : Ti-Diopside = CaTiAl<sub>2</sub>O<sub>6</sub>, Aegirine = NaFe<sup>3+</sup>Si<sub>2</sub>O<sub>6</sub>, Tschermakite = CaAl<sub>2</sub>SiO<sub>6</sub>, Hedenbergite = CaFe<sup>2+</sup>Si<sub>2</sub>O<sub>6</sub>, Diopside = CaMgSi<sub>2</sub>O<sub>6</sub>, Kanoite = MnMgSi<sub>2</sub>O<sub>6</sub>, Clinoenstatite = Mg<sub>2</sub>Si<sub>2</sub>O<sub>6</sub>.

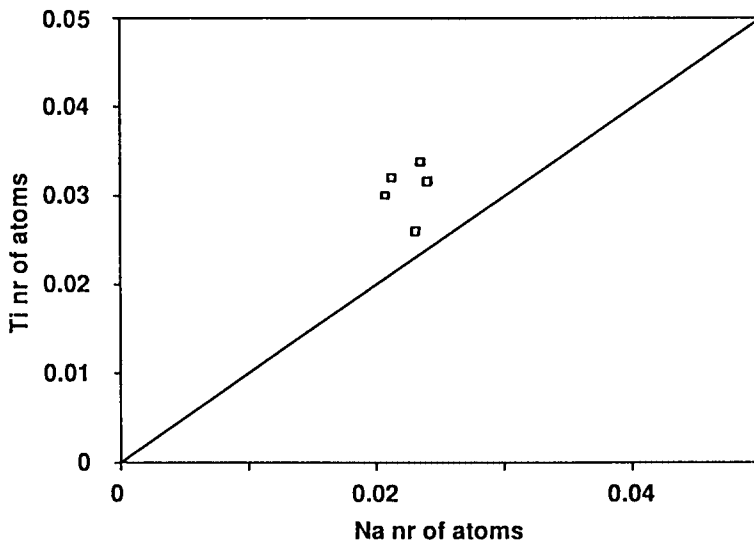


Fig. 1. G/17-2 clinopyroxenes, Atom ratios Na vs. Ti.

EPMA results on five clinopyroxene grains are given in Table 2, together with atomic ratios calculated on the basis of four cations (Vieten & Hamm, 1978; Morimoto et al., 1988). From Table 2 it is apparent that the clinopyroxenes show a relatively strong variability in chemical composition.

As EPMA does not give results for  $\text{Fe}^{3+}$  but rather treats all Fe as being  $\text{Fe}^{2+}$ , the calculation of end-member ratios is not straightforward, especially so since vacant sites can occur within the clinopyroxene lattice (Mysen & Griffin, 1973; Vieten & Hamm, 1978). Assuming stoichiometry and under reasonable assumptions of analytical precision and accuracy, the following can be inferred:

All pyroxenes are relatively silica-undersaturated with Si below or equal to 1.90. Consequently, a substantial substitution of  $\text{Al}^{\text{IV}}$  for Si must have taken place on the tetrahedral site (T-position).

In the model calculation, sufficient four-coordinated Al ( $\text{Al}^{\text{IV}}$ ) is allocated to the T-position to fill this site together with Si to 2.0. The remaining Al then is VI-coordinated on one of the octahedral sites ( $\text{M}_1$ ).

As there is no correlation between Ti and Na (Fig. 1), Na-Ti end-members are not likely to be present and all Ti may be taken as Ti-diopside ( $\text{CaTiAl}_2^{\text{IV}}\text{O}_6$ ). From the Al/Ti ratio, which ranges from 4 to 5, it is apparent that the pyroxenes contain more Al than necessary to balance the Ti in Ti-diopside. Also, there exists a negative correlation between  $\text{Al}_2\text{O}_3$  (Wt.%) and Fe as FeO and MgO, respectively.

In view of the foregoing, the  $\text{Al}^{\text{IV}}$  remaining after allowing for Ti-diopside is taken as Calcium-Tschermak's molecule ( $\text{CaAl}^{\text{VI}}\text{Al}^{\text{IV}}\text{SiO}_6$ ). As there is insufficient  $\text{Al}^{\text{VI}}$  to balance  $\text{Al}^{\text{IV}}$  in the tschermakite, all Cr is taken to substitute on the octahedral site  $\text{M}_1$ . This still does not balance  $\text{Al}^{\text{IV}}$  and sufficient Fe is taken as  $\text{Fe}^{3+}$  to fill up this octahedral site.

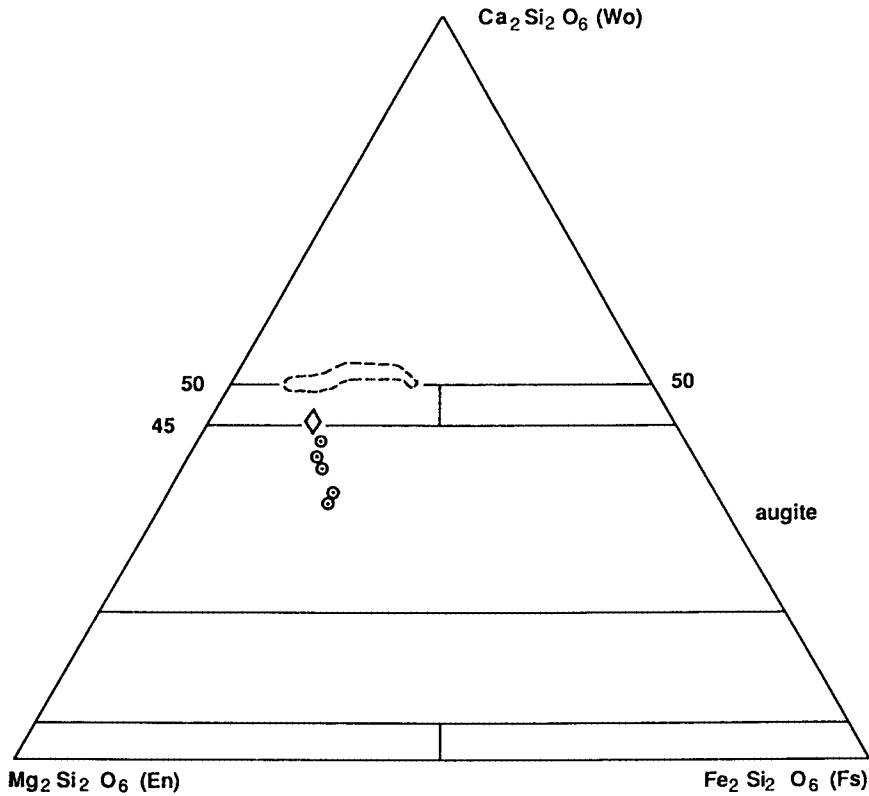


Fig. 2. G/17-2 clinopyroxenes, Ca-Mg-Fe triangular diagram.

- = G/17-2 clinopyroxenes;
- ⊖ = pyroxenes from Jurassic-Cretaceous undersaturated basaltic rocks (Dixon et al., 1981);
- ◇ = pyroxenes from Permian basaltic rocks (Dixon et al., 1981).

The insufficient amount of  $Al^{VI}$  combined with the excess  $Al^{IV}$ , which can only be accommodated in tschermakite, indicates that Na cannot be present as jadeite ( $NaAlSi_2O_6$ ), but has to reside in the aegirine end-member ( $NaFe^{3+}Si_2O_6$ ). Accordingly, sufficient Fe is taken as  $Fe^{3+}$  to balance Na in aegirine. The remaining Fe is taken as  $Fe^{2+}$  in hedenbergite ( $CaFe^{2+}Si_2O_6$ ); the Ca remaining after this step is taken as diopside ( $CaMgSi_2O_6$ ), Mn is taken as kanoite ( $MnMgSi_2O_6$ ), and finally, the excess Mg is taken as clinoenstatite ( $Mg_2Si_2O_6$ ).

The end-member ratios calculated according to the above allocations are given in Table 2. When plotted in the Q-J diagram ( $Q = Ca + Mg + Fe^{2+}$ ,  $J = 2Na$ ; Morimoto et al., 1988), all clinopyroxenes fall in the field of normal Ca-Mg-Fe pyroxenes. In the Ca-Mg-Fe triangular diagram, the clinopyroxenes plot in the augite field, and can be classified as normal to slightly calcic augites (Fig. 2).

Table 3. Olivine composition.

	OI-A	OI-B	OI-C
<b>Wt.% oxide</b>			
SiO <sub>2</sub>	35.50	34.70	36.10
Al <sub>2</sub> O <sub>3</sub>	0.05	0.05	0.00
TiO <sub>2</sub>	0.05	0.07	0.00
FeO	34.80	36.70	32.60
MnO	0.57	0.64	0.50
MgO	28.60	26.70	30.40
NiO	0.11	0.11	0.13
CaO	0.24	0.27	0.29
Total	99.92	99.24	100.02
<b>Atomic ratios</b>			
Si	0.988	0.984	0.992
Al	0.002	0.002	0.000
Ti	0.001	0.002	0.000
Fe	0.810	0.871	0.749
Mg	1.186	1.129	1.245
Mn	0.013	0.015	0.012
Ni	0.003	0.003	0.003
Ca	0.007	0.008	0.009

### *Olivines*

EPMA results on three olivine grains are given in Table 3. The atomic ratios were calculated on the basis of four oxygen. Forsterite percentages range from 56 to 62, slightly lower than indicated by the optical properties. The minor and trace element contents fall within the range for normal olivine (Kuijper, 1979; Brown, 1980).

### *Plagioclase*

Table 4 gives EPMA results on plagioclase cores and rims. The atomic ratios were calculated on the basis of eight oxygen. Anorthite percentages in the cores range from 42 to 76, while those in the rims vary between 37 and 71. The orthoclase percentages are negatively correlated to the anorthite-content and range from 0.1 to 3.6.

The chemical zonation of the plagioclase can be explained by competition with clinopyroxene for the chemical components. Early plagioclase is An-rich, and will have shifted the melt towards a lower Al content. As soon as clinopyroxene started to crystallize, however, both plagioclase and clinopyroxene competed for CaAlAlSiO<sub>6</sub>, and consequently the later plagioclase (rims) is less enriched in An.

## Mineral composition and emplacement of the dolerite

From the absence of quench textures, a minimum depth of emplacement of a few tens to perhaps a few hundreds of metres can be inferred. Regional seismic and

Table 4. Plagioclase composition.

	A core	A rim	B core	B rim	C core	C rim	D rim	E	F core	F rim
Wt.% oxide										
SiO <sub>2</sub>	57.10	57.90	50.30	57.60	8.20	49.30	56.40	50.90	52.40	51.70
Al <sub>2</sub> O <sub>3</sub>	25.70	25.80	30.60	25.10	31.00	30.40	25.70	29.40	28.40	28.60
FeO	0.77	0.77	0.69	0.65	0.62	0.69	1.05	0.77	0.79	0.88
CaO	8.95	8.38	14.10	7.87	15.30	14.70	8.88	13.60	12.20	12.70
Na <sub>2</sub> O	6.42	6.75	3.45	6.90	2.68	3.23	5.93	3.78	4.75	4.35
K <sub>2</sub> O	0.54	0.59	0.14	0.64	0.08	0.13	0.48	0.17	0.21	0.17
Total	99.48	100.19	99.28	98.76	97.88	98.45	98.44	98.62	98.75	98.40
Atomic ratios										
Si	2.589	2.603	2.315	2.623	2.258	2.295	2.583	2.357	2.416	2.396
Al	1.373	1.367	1.660	1.347	1.712	1.668	1.387	1.605	1.544	1.562
Fe	0.029	0.029	0.027	0.025	0.024	0.027	0.040	0.030	0.031	0.034
Ca	0.435	0.404	0.695	0.384	0.768	0.733	0.436	0.675	0.603	0.630
Na	0.565	0.589	0.308	0.610	0.244	0.292	0.527	0.340	0.425	0.392
K	0.031	0.034	0.008	0.037	0.005	0.008	0.028	0.010	0.012	0.010

maturation data indicate that the current depth may more or less be regarded as the maximum depth. Wall-rock temperature at the time of emplacement thus may be estimated at 50-120°C.

The atomic and end-member ratio calculation of the clinopyroxene is strongly dependent on the analytical uncertainty. The precision and accuracy of EPMA is generally lowest for Si-determination. The allocation of Al to Al<sup>IV</sup> and subsequent allocation of Fe to Fe<sup>3+</sup> thus depends strongly on the uncertainty of the Si-value. Still, taking into account the analytical error, the Ti/Al ratio is relatively low, while the Al<sup>IV</sup>/Al<sup>VI</sup> ratio is high. A low Ti/Al ratio is indicative for rapid cooling (Mevel & Velde, 1976).

Experimental studies on clinopyroxene crystallization and analytical data from natural clinopyroxenes have shown a clear pressure dependence of Al-coordination in clinopyroxenes, decreasing pressure leading towards higher Al<sup>IV</sup>/Al<sup>VI</sup> ratios (Wass, 1979). The high Al<sup>IV</sup>/Al<sup>VI</sup> ratio of the G/17-2 pyroxenes thus concurs with the limited depth of emplacement and hence the limited confining pressure, roughly 1 kb at the most. In the absence of WR chemical analyses, however, the Al<sup>IV</sup>/Al<sup>VI</sup> ratio cannot be used as a geobarometer in this case.

In coexisting clinopyroxene-olivine, Fe<sup>2+</sup> has a preference for the olivine. The Fe/Mg partitioning of this mineral pair is dependent on temperature and may be used as a geothermometer. Using the formula of Powell & Powell (1974) and the atomic ratios of Tables 2 and 3, an average emplacement temperature of 1265 K (992°C) is calculated. In view of the analytical uncertainty and the dependence of the formula on Fe and Al allocation, calculations were also made using all Al as Al<sup>VI</sup> and all Fe as Fe<sup>2+</sup>. The resulting temperatures are less than 1.5% higher than the calculated 1265 K.

Some remarks have been made on the validity of this geothermometer (Brown, 1980), especially with regard to the limited range of calibration temperatures used (1300-1500 K). However, the T calculated for the G/17-2 dolerite is sufficiently close to this range that it may be assumed to be within 10% of the actual T of equilibration.

The above temperature of c. 1000°C ( $\pm 100$ ) should be regarded as the T at which ion-exchange between olivine and clinopyroxene stopped. The intrusion T will have been higher and in the absence of phenocrysts and flow orientation of crystals it may be inferred that intrusion took place as a liquid at or above liquidus temperatures. At low pressure, the liquidus T of dry basaltic/gabbroic melts is 1200-1250°C. On the one hand, as the melt will have originated at greater depth, the intrusion temperature might very well have been higher. On the other hand, introduction of some fluid phase will have lowered the liquidus T. In the absence of whole-rock chemical analyses then, the intrusion T can only be estimated at 1100-1400°C.

### Thermal disturbance of the surrounding sediments

The emplacement of the G/17-2 dolerite at over 1000°C within a country rock with ambient T of 50-120°C will have resulted in a disturbance of the local geothermal gradient. The extent and the decay-time of this disturbance will depend on the amount of heat released by the intrusive body and on the heat-capacity and conductivity of the wall-rock (Jaeger, 1957).

The dolerite itself will have solidified rather rapidly. Using a thickness (D) of 14 m and a time-span for complete solidification of  $0.010 D^2 - 0.915 D^2$  years, the lapse of time between intrusion and solidification may be estimated at 2-3 years. This estimate probably represents a maximum as the model calculations have been performed mostly on systems where the temperature difference between intrusive mass and wall-rock is much less than in the G/17-2 case.

Taking the intrusion T of the G/17-2 dolerite at 1400-1100°C and the solidus at a maximum of 1000°C (the olivine-clinopyroxene equilibration T calculated above), the temperature at the intrusive contact may be estimated at 825-656°C, depending on the crystallization range and the latent heat of crystallization. At the low P of emplacement, this will have been too low to induce partial melting of the surrounding sediments, but could be high enough to result in various mineral reactions, if sufficient heat would be released.

Taking  $\rho = 2.8$ , the latent heat of crystallization  $L = 418$  J/g, the specific heat capacity of the liquid magma = 1.26 J/g°C, and the specific heat capacity of the solidified dolerite = 1.05 J/g°C, the maximum amount of heat released by 1 m<sup>3</sup> of dolerite, intruding at 1400°C, solidifying and cooling to 1000°C amounts to about  $5 \times 10^9$  J. Taking into account the strong decrease of specific heat capacity of pyroxene at lower T's, this maximum might even be lowered to about  $3 \times 10^9$  J (Powell, 1978; Fei & Saxena, 1987). Evidently, only part of this heat is used to heat the country rock immediately adjacent to the dolerite, as the contact T is only of the order 600-800°C. Cooling to this range provides a maximum amount of some  $3 \times 10^9$  J.

The T profile away from the intrusive contact strongly depends on the thermal conductivity of the Upper Carboniferous sediments. In a layered and/or foliated sequence, the thermal conductivity parallel to the layering/foliation is much higher than normal to it (Talbot, 1971). If the G/17-2 dolerite intruded more or less parallel to the sedimentary layering, the T profile should have been quite steep. Even then, after a very limited number of years (<10), the temperature at the intrusive contact should have dropped by >200°C. As no data on the conductivity and especially the conductivity-anisotropy of the Carboniferous sediments are at hand, the T profile cannot be calculated. The limited thickness of the intrusion, however, will have resulted in only a limited extent of the thermal anomaly (Jaeger, 1957).

Based on the above qualitative approach and the estimated contact temperature, it may be stated that the excess heat produced by the G/17-2 dolerite has probably resulted in thermal cracking of all kerogen in the immediate vicinity of the intrusion. Away from the contact, however, it could have given rise to an increase in maturation, as for a limited number of years a temperature of over 200°C could be maintained at distances up to 100 m from the contact. In view of the small size of the intrusion, this effect will likewise have been small, and certainly not of the extent as found near the East Groningen Massif (Kettel, 1983).

The effect, however, might be large enough to result in a noticeable departure from linear behaviour of the maturation profile. Normally, such departure would be interpreted as resulting from tectonic activity (e.g. faulting or inversion/erosion). Here it is shown that care should be taken in such interpretations as nearby intrusions may give rise to similar anomalies.

## Discussion

In the absence of isotopic age data, little can be said on the timing of the intrusive event. Evidently, the dolerite is post Late Carboniferous, but a younger time-limit is impossible to assess.

Igneous activity has been recorded from several intervals of the North Sea Basin evolution. During the latest Carboniferous and Early Permian, alkaline bimodal magmatism occurred associated with faulting and probably pull-apart structures. A trend towards more calc-alkaline compositions has been discerned in the southern part of the North Sea Basin. In the Middle Jurassic, alkaline bimodal magmatism occurred at the Central Graben - Viking Graben - Moray Firth junction. Late Jurassic - Early Cretaceous alkaline volcanism was associated with the Late Cimmerian phase of tectonic activity. In the Tertiary, episodic magmatism occurred during the Paleocene-Eocene and the Oligocene-Miocene (Ronsbo et al., 1977; Ziegler, 1982; Glennie, 1986; Shannon & Naylor, 1989).

As the sample size not only precluded isotopic age dating but also whole-rock major and trace element analysis, it is virtually impossible to definitely relate the G/17-2 dolerite to any of these magmatic events.

The G/17-2 dolerite is less altered than nearly all the other igneous rocks encountered in the Netherlands subsurface, no albitization has taken place, and carbonatization is minimal. However, differences in degree of alteration cannot be

regarded as reflecting differences in age of emplacement.

The G/17-2 clinopyroxenes clearly differ from those of the Jurassic-Cretaceous undersaturated alkaline basaltic rocks. The latter are calcic augites and in the Ca-Mg-Fe triangular diagram plot on or above the 50%  $\text{Ca}_2\text{Si}_2\text{O}_6$  line (Fig. 2), from which either a high johannsenite ( $\text{CaMnSi}_2\text{O}_6$ ) content or an unusual pyroxene composition can be inferred (Morimoto et al., 1988). The difference between the G/17-2 clinopyroxenes and those of Permian basaltic rocks from the northern flank of the Ringkobing-Fyn High is less striking. The G/17-2 pyroxenes are slightly less calcic and straddle the Skaergaard tholeiitic trend (Dixon et al., 1981).

Combining the modal composition and the mineral analyses, it may be suggested that the G/17-2 dolerite is mildly undersaturated and relatively Fe-poor and Ca-rich.

The above inferences would indicate that the G/17-2 dolerite is more closely related to the Permian magmatism than to the Jurassic-Cretaceous magmatic events. However, it should be stressed that this relationship is quite uncertain and as such no definite age-brackets can be given.

## References

- Brown Jr., G.E., 1980. Olivines and Silicate spinels. – *Reviews in Mineralogy*, Vol.5, Orthosilicates, Min. Soc. America: 275-381.
- Dixon, J.E., J.G. Fitton & R.T.C. Frost, 1981. The tectonic significance of post-Carboniferous igneous activity in the North Sea Basin. In: L.V. Illing & G.D. Hobson (eds) *Petroleum Geology of the Continental Shelf of NW Europe* – Inst. Petr., London: 121-137.
- Fei, Y. & S.K. Saxena, 1987. An equation for heat capacity of solids. – *Geoch. Cosm. Acta*, 51: 251-254.
- Glennie, K. W., 1986. Development of N.W. Europe's Southern Permian Gas Basin. In: J. Brooks, J. Goff & B. van Hoome (eds) *Habitat of Paleozoic Gas in N.W. Europe* – *Geol. Soc. Spec. Publ.*, 23: 3-22.
- Jaeger, J.C., 1957. The temperature in the neighbourhood of a cooling intrusive sheet. – *Am. J. Sci.*, 255: 306-318.
- Kettel, D., 1983. The East Groningen Massif - detection of an intrusive body by means of coalification. – *Geol. Mijnbouw*, 62: 203-210.
- Kimpe, W.F.M., 1953. Doleritic and gabbroic intrusives in the Autunian (Lower Permian) of the boring Wanneperveen I, Eastern Netherlands. – *Geol. Mijnbouw*, 15: 57-65.
- Kuijper, R.P., 1979. Olivine with perfect cleavage. – *N. Jb. Miner. Mh.*, 1979: 10-16.
- Mével, C. & D. Velde, 1976. Clinopyroxene in Mesozoic pillow lavas from the French Alps: Influence of cooling rate on compositional trends. – *Earth Planet. Sci. Lett.*, 32: 158-164.
- Morimoto, N., J. Fabries, A.K. Ferguson, I.V. Ginzburg, M. Ross, F.A. Seifert, J. Zussman, K. Aoki & G. Gottardi, 1988. Nomenclature of Pyroxenes. – *Schweiz. Miner. Petrogr. Mitt.*, 68: 95-111.
- Mysen, S. & W.L. Griffin, 1973. Pyroxene stoichiometry and the breakdown of omphacite. – *Am. Miner.*, 58: 60-63.
- NAM & RGD (Nederlandse Aardolie Maatschappij B.V. & Rijks Geologische Dienst), 1980. *Stratigraphic Nomenclature of the Netherlands*. – *Verh. Kon. Ned. Geol. Mijnbouw. Gen.*, 32: 1-77, 33 enclosures.
- Perrot, J. & A.B. van der Poel, 1987. Zuidwal - a Neocomian gasfield. In: J. Brooks & K.W. Glennie (eds) *Petroleum Geology of N.W. Europe*. – Graham & Trotman, London: 325-335.
- Powell, R. 1978. *Equilibrium Thermodynamics in Petrology*. – Harper & Row, London: 1-284.

- Powell, M. & R. Powell, 1974. An olivine-clinopyroxene geothermometer. – *Contr. Miner. Petr.*, 48: 249-263.
- Ronsbo, J.G., A.K. Pedersen & J. Eugell, 1977. Titan-aegirine from early Tertiary ash layers in northern Denmark. – *Lithos*, 10: 193-204.
- Shannon, P.M. & D. Naylor, 1989. *Petroleum Basin Studies*. – Graham & Trotman, London: 1-206.
- Sijp, J.W.C.M. van der, 1953. Intrusive rocks in the Berkel well. – *Geol. Mijnbouw*, 15: 65-66.
- Talbot, J.C., 1971. Thermal convection below the solidus in a mantled gneiss dome, Fungwi reserve, Rhodesia. – *J. Geol. Soc.*, 127: 377-410.
- Taylor, J.C.M., 1983. Bit-metamorphism, illustrated by lithological data from German North Sea wells. – *Geol. Mijnbouw*, 62: 211-219.
- Vieten, K. & H.M. Hamm, 1978. Additional notes "On the calculation of the crystal chemical formula of clinopyroxenes and their contents of Fe<sup>3+</sup> from microprobe analyses". – *N. Jb. Miner. Mh.*, 1978: 71-83.
- Voorthuysen, J.H. van, 1944. Hoornblendediabaas-intrusie in het Wealden van Oostnederland. – *Geol. Mijnbouw, N.S.*, 6: 24-26.
- Wass, S.Y., 1979. Multiple origins of clinopyroxenes in alkali basaltic rocks. – *Lithos*, 12: 115-132.
- Ziegler, P. A., 1982. *Geological Atlas of Western and Central Europe*. – Shell Internationale Petroleum Mij B.V., The Hague.

Manuscript received 18 October 1990.